Supplementary Information

For

Quantitative Affinity Determination by Fluorescence Anisotropy Measurements of Individual Nanoliter Droplets

Fabrice Gielen[†#], Maren Butz[†,#,$], Eric J. Rees[‡], Miklos Erdelyi[‡⊥], Tommaso Moschetti[†], Marko Hyvonen[†], Joshua B. Edel[§], Clemens F. Kaminski[‡], Florian Hollfelder[*,†]

[†] *Department of Biochemistry, University of Cambridge, 80 Tennis Court Road, Cambridge, CB2 1GA, UK*
[‡] *Department of Chemical Engineering and Biotechnology, New Museums Site, Pembroke Street, Cambridge, CB2 3RA, UK*
[⊥] *Department of Optics and Quantum Electronics, Szeged, Dom ter 9, Hungary*
[§] *Department of Chemistry, Imperial College London, South Kensington, London, SW7 2AZ, UK*
[$] *Present address: AstraZeneca, Innovative Medicines Discovery Science, Mereside, Alderley Park, Macclesfield, Cheshire SK10 4TG, UK*

[#] Denotes equal contribution

Table of Contents

S1. G-factor correction

The G-factor represents the ratio of the detection sensitivities of the detector. A G-factor calibration image was acquired at the start of a day of experiment. 10 µL of a 1 µM pure aqueous fluorescein solution was pipetted on a custom-made well bonded on a thin cover slide (thickness 130 µm). 1000 frames were accumulated with an exposure time of 0.03 seconds. The formula used to plot G pixel-by-pixel is equation 2 in the main text. In a perfect setup, G should be close to 1 for each pixel. However, as seen in Figure S1, there is a discrepancy up to 20% at the bottom left of the image compared to the top right, which has values close to 1.

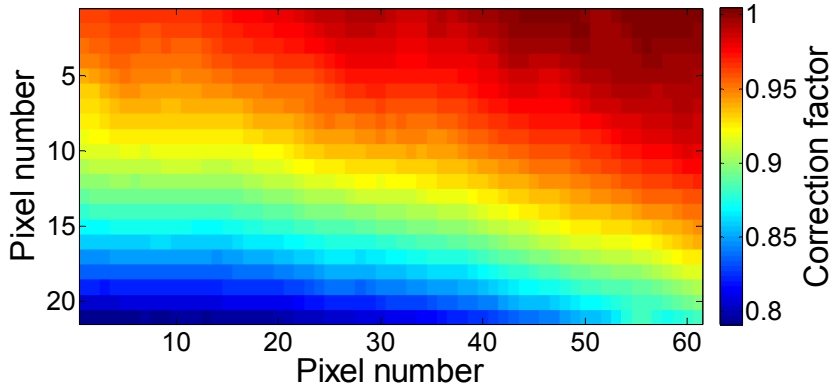

Figure S1. *G-factor image used for calibrating anisotropy measurements.* The map was obtained with a 1 µM fluorescein solution in water. Figure S3 was obtained by division of the parallel and perpendicular intensity maps (c.f. Figure 2).

S2. Experimental set-up

Figure S1A displays a photograph of the microfluidic set-up comprising two multirack syringe pumps (Chemyx Fusion 200 and Chemyx Nexus 3000). Each droplet maker is controlled with a separate glass syringe (SGE, gas tight, 100 µL) connected to one channel of the microfluidic chip (Figure S1B). The corresponding PTFE tubing (I.D. 200 µm, O.D. 400 µm) is then put into a custom-built adapter for generating droplets from a well of a 384 well plate (Figure S1C). Each well contains a magnet (Fisher Scientific, 2x2 mm) and the 384 well-plate stands on a magnetic stirring plate. The distance from the well plate to the chip was around 30 cm.

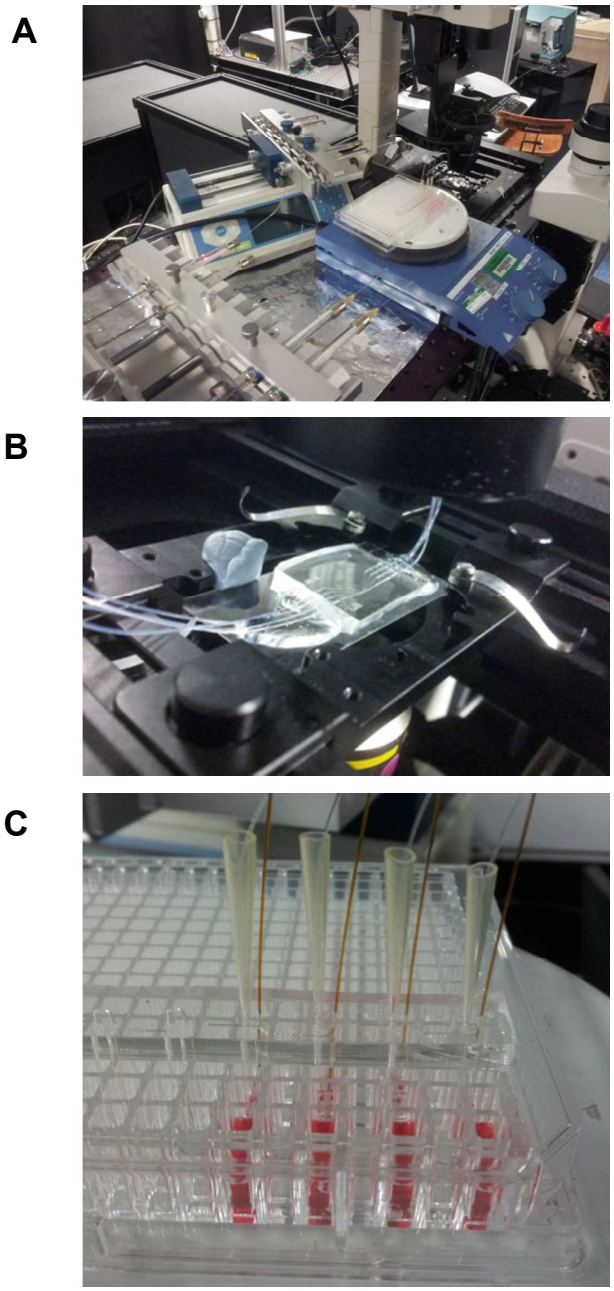

Figure S2. *Photographs of the microfluidic setup* **(A)** A multirack syringe pump (at the back) provides negative pressure for droplet formation and a magnetic stirrer was used to mix microwell contents. The reagents were infused using a second multirack syringe pump (at the front). Droplets formed were measured in-line with a fluorescence anisotropy microscope. **(B)** A microfluidic device with four parallel channels sits on the stage of the microscope. PTFE tubings connect one side of the microchannel to the withdrawing pump and the other side to the droplet making head **(C)** The droplet making head. PTFE tubings were fitted into a custom-built adapter for generating droplets from open microwells of a 384 well plate. For gradient generation, silica capillaries were used to infuse a second component to the wells.

S3. Microfluidic device designs

Microfluidic devices were built by classical soft lithography.[1-3] Devices had rectangular channels (height 200 µm). The single channel configuration had a width of 150 microns (Figure S2A), while each of the four channel configuration had a width of 80 µm and a gap between channels of 50 µm (Figure S2B and S2C).

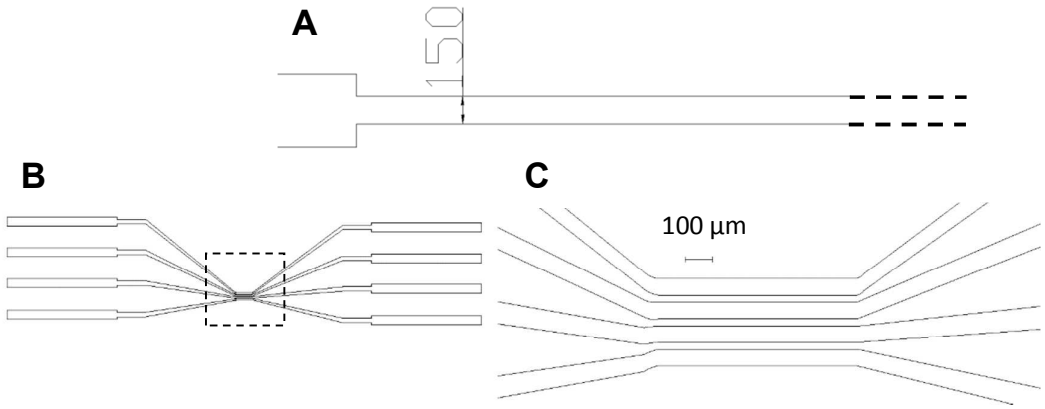

Figure S3. *Designs of the microfluidic devices* **(A)** Single channel design. **(B)** Parallel design with four inlets and four outlets in line. **(C)** Close-up of the converging area where the 4 channels meet.

S4. Extracting concentrations from time-tagged droplets

Concentrations for each droplet were derived using the fluidic parameters (initial volume V_i, flow rates of infusion and withdrawal (q_{in} and q_{out})) and the time of generation t using equation S1:

$$c_2(t) = c_{2,i}\left[1 - \left(\frac{V_i}{(V_i + (q_{in} - q_{out})t)}\right)^{\left(\frac{q_{in}}{q_{in} - q_{out}}\right)}\right] \quad \text{(eq. S1)}$$

where $c_{2,i}$ is the initial reagent concentration

S5. BSA titration

BRC4^{fl} was found to have a high propensity for leakage, when using HFE 7500 with 1% w/v AZ2C fluoro-surfactant (made in-house according to a previously published method).[4] The time to reach the detection point (approx. 1 minute) was sufficient for significant leakage of BRC4^{fl} from the droplet. Addition of additives such as BSA has been found effective in increasing the effective solubility of reagents.[5] BSA was titrated using the same droplet titration technique up to 1.2%. The fluorescence intensity measured at the detection point was seen linearly increasing with increasing BSA contest, suggesting that the BSA does indeed increase retention of the fluorophore in the droplet. Anisotropy reached a steady-state value when BSA was present at concentrations above 0.2%. Although the linear increase of fluorescence suggests there is still some labelled peptide leaking from the droplet, the presence of BSA concentrations above 1% made droplet formation more difficult, because of the increased viscosity of the aqueous phase and the formation of BSA vesicles. Therefore 1% BSA was chosen as a compromise between these effects and all experiments were performed in this way.

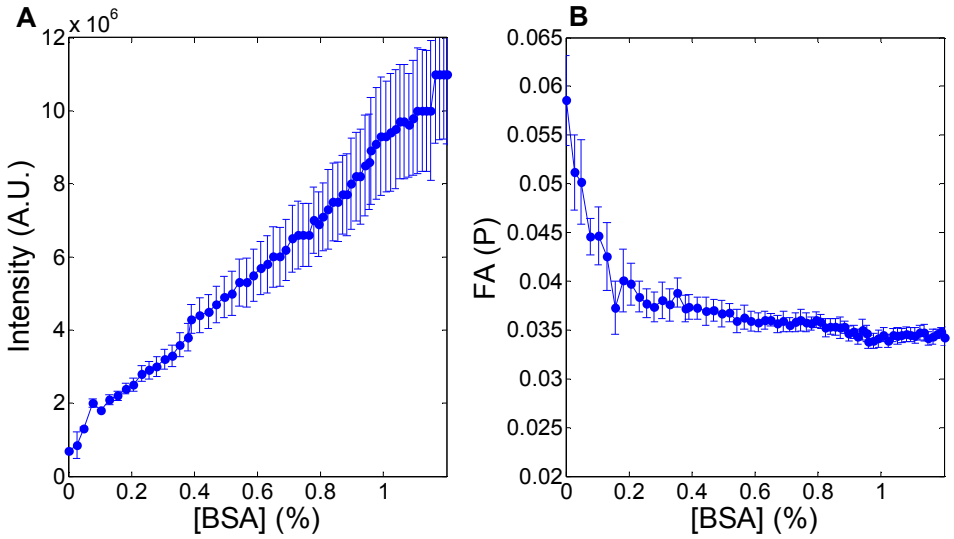

Figure S4. *Influence of BSA concentration on the retention of BRC4^{fl} within the droplet.* **(A)** Intensity is linearly increasing with BSA concentration. **(B)** Fluorescence anisotropy converges towards a steady-state value above a threshold concentration of BSA

S6. Anisotropy stability at different concentrations of BRC4

We characterized the change in measured anisotropy depending on the initial concentration of freely floating labelled ligand at constant laser powers (5, 10 and 50 mW) using a 20x objective. Therefore, we injected continuously 60 µL of buffer into a 30 µL solution containing 40 nM and 100 nM $BRC4^{fl}$ (for 10 mW and 5 mW, respectively). For the 50 mW, we injected 40 µL 40 nM $BRC4^{fl}$ into 40 µL buffer. All curves were obtained using CHES buffer pH 9.5 with 0.2 % BSA.

The anisotropy remains near-constant, but increases slightly when diluted 4-fold from the respective initial concentrations. Concentrations higher than 20, 40, and 100 nM $BRC4^{fl}$ resulted in significant parts of the image being saturated using 5, 10, and 50 mW, respectively. The limit of fluorescence detection at 50 mW laser power to get an accurate anisotropy estimate was around 5 nM $BRC4^{fl}$.

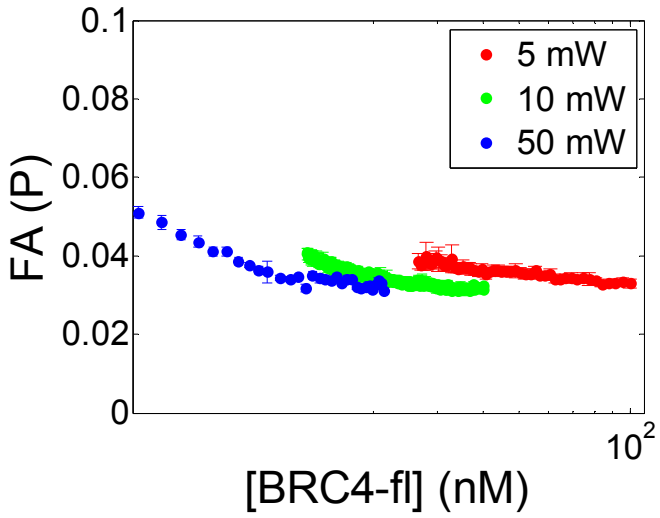

Figure S5. Anisotropy read-out for dilutions of $BRC4^{fl}$ at three different laser powers (5, 10 and 50 mW).

S7. Influence of the focal plane

The average anisotropy per droplet was measured when focussing at different height within and outside the microchannel. The anisotropy reaches a minimum for unbound BRC4-fluorescein close to the intensity maximum, indicating the best place for measurement. Outside the channel, anisotropy increases probably due to scattering or non-uniform dye distribution within a plug. This is shown in Figure S6.

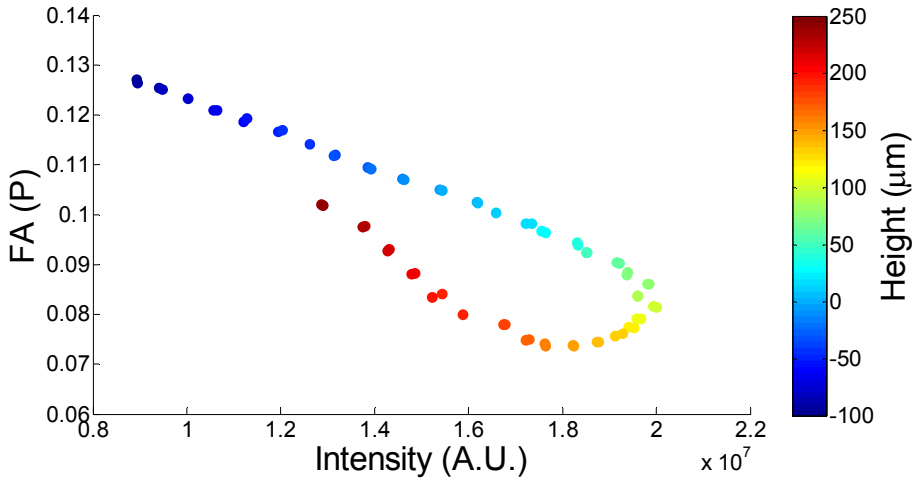

Figure S6. *Measuring anisotropy of the same droplets at different focal planes.* The cover glass slide was chosen to be the reference focal plane of 0 μm. The sample was 5 nM $BRC4^{fl}$ with 30% cell lysate and 1% BSA.

In order to evaluate the error made by measuring at different focal planes, a full titration of HumRadA18 against $BRC4^{fl}$ was measured at different focussing points. The resulting curves are shown in Figure S7. The absolute anisotropy values for the different titrations get shifted but the normalization to the minimum anisotropy read-out (Figure S7B) shows that the dynamic range is preserved for a wide range of focal planes. The decrease in dynamic range between focussing at the exact centre of the channel (~110 μm) or 80 microns above is 5%. This implies manual focussing is not deleterious to the final sensitivity of the measurements and can be reproduced fairly simply.

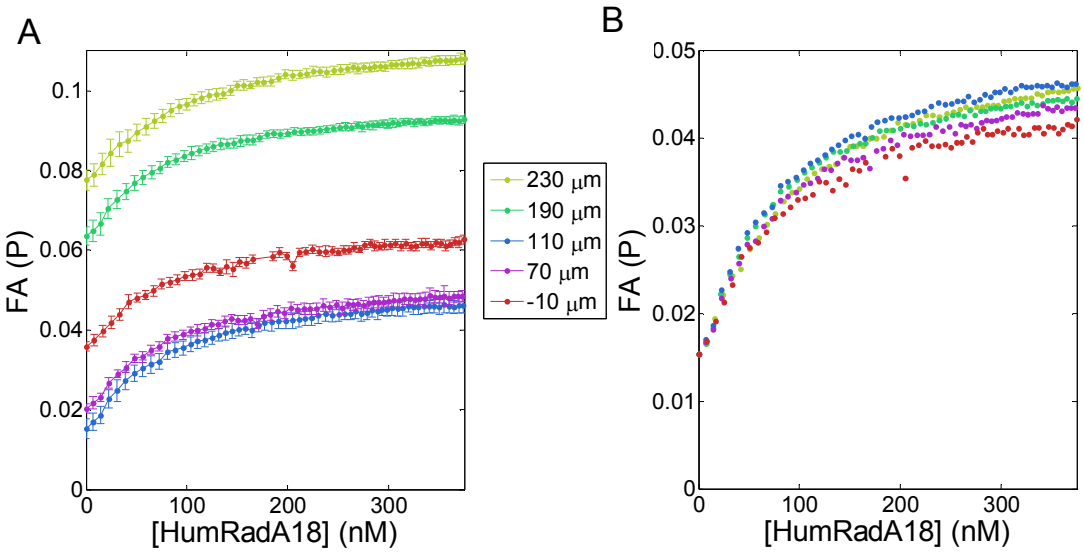

Figure S7. *Measurement of a titration at different focal planes* (**A**) HumRadA18-BRC4^{fl} titration measured at different focal planes. A reference focal plane of 0 μm was chosen to be the cover glass slide. (**B**) Titrations normalized for starting anisotropy offset.

S8. Anisotropy imaging - error analysis

Droplets were typically flown at 3 µL/min with a generation rate of ~2 Hz resulting in around 40-60 frames per droplets.

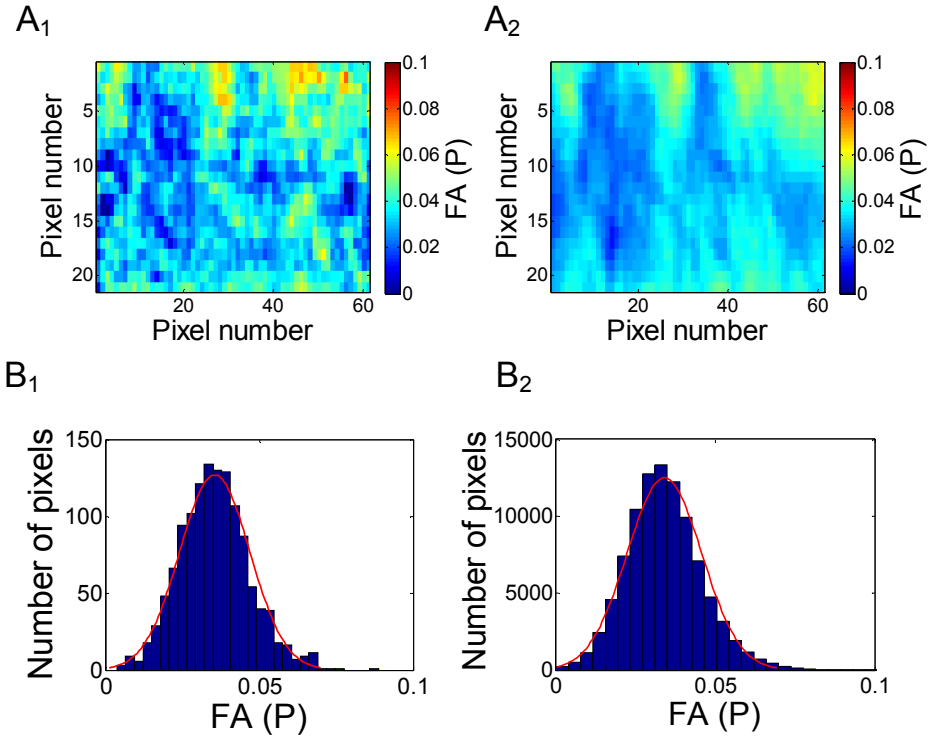

Figure S8. *Comparison of data extracted between a single frame (1) and accumulated 70 frames (2)*. **(A_1** and **A_2)** Mean anisotropy maps and corresponding histograms **(B_1** and **B_2)** measured from a single frame versus mean anisotropy from 70 accumulated frames of the same droplet. Maps correspond to a large rectangular area as shown in Figure $3A_1$.

	Single frame	**All frames**
Mean anisotropy	35.5 ± 11.9 mP	34.0 ± 8.4 mP

A high number of accumulated frames (70) only slightly increased the accuracy of the measurement. Therefore, the main remaining source of systematic error must be ascribed to instrument calibration. Likewise averaging over many droplets will not result in more accurate quantification.

S9 Cell lysate titrations

We have performed a negative control by infusing cell lysate prepared in typical conditions pre-mixed with 100 nM BRC4^{fl} into a well containing 100 nM BRC4^{fl}. The anisotropy was found not to change over the course of the titration within sensitivity limits for 100 nM BRC4fl indicating no detectable non-specific interactions between BRC4^{fl} and other cellular components. For 20 nM BRC4^{fl}, a slight increase in FA signal can be seen but still amounts to less than 10% the dynamic range of the assay.

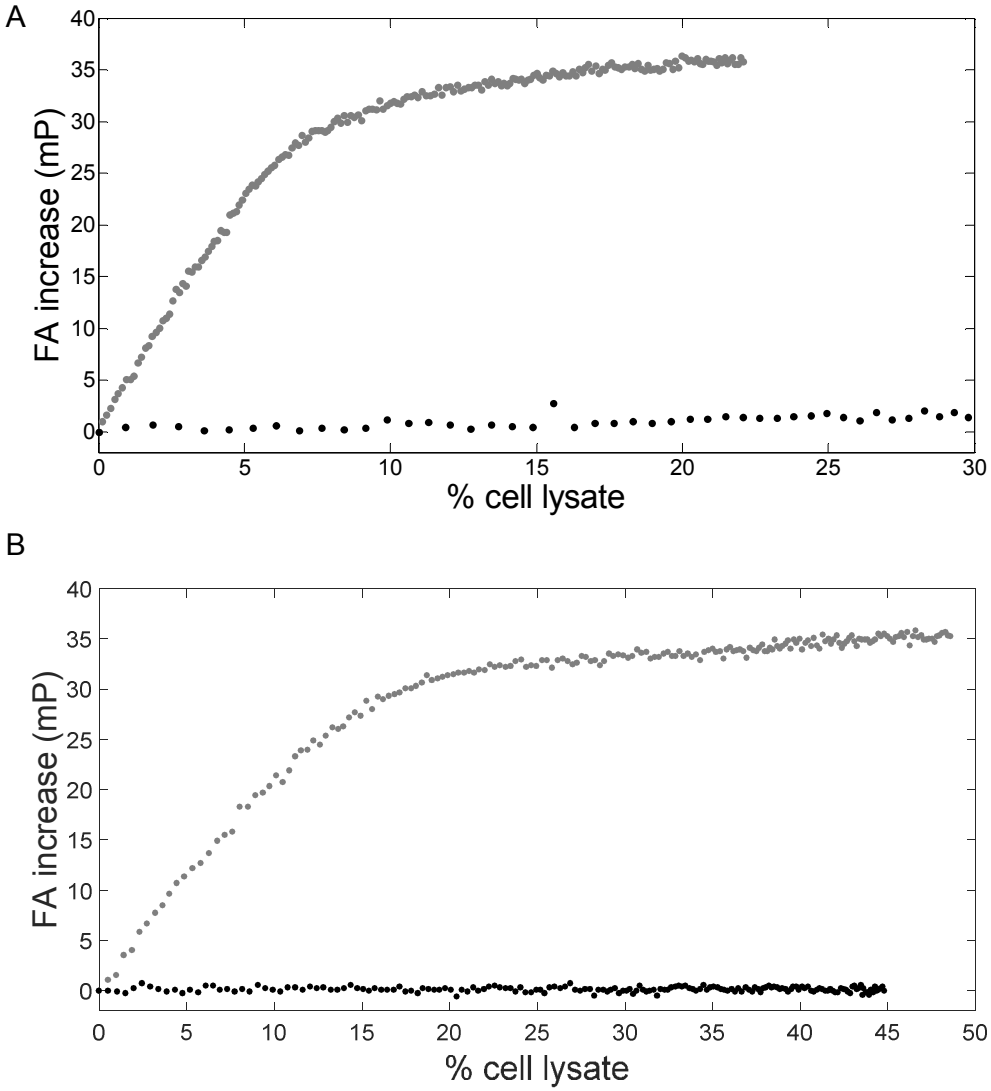

Figure S9. FA increase versus amount of control cell lysate not expressing any HumRadA (black dots) for 20 nM BRC4^{fl} (A) and 100 nM BRC4^{fl} (B) overlayed with HumRadA22 titrations (grey dots) at 20 nM (A) and 100 nM BRC4^{fl} (B) respectively.

S10. Fits of anisotropy data obtained in lysate screens

Figure S10 displays raw titration data for all HumRadA variants in lysates tested at two concentrations of $BRC4^{fl}$: 20 nM (red) and 100 nM (blue) for HumRadA14, HumRadA16, HumRadA18 and HumRadA22, respectively. For HumRadA20, the concentrations were 5 nM $BRC4^{fl}$ (red) and 100 nM (blue).

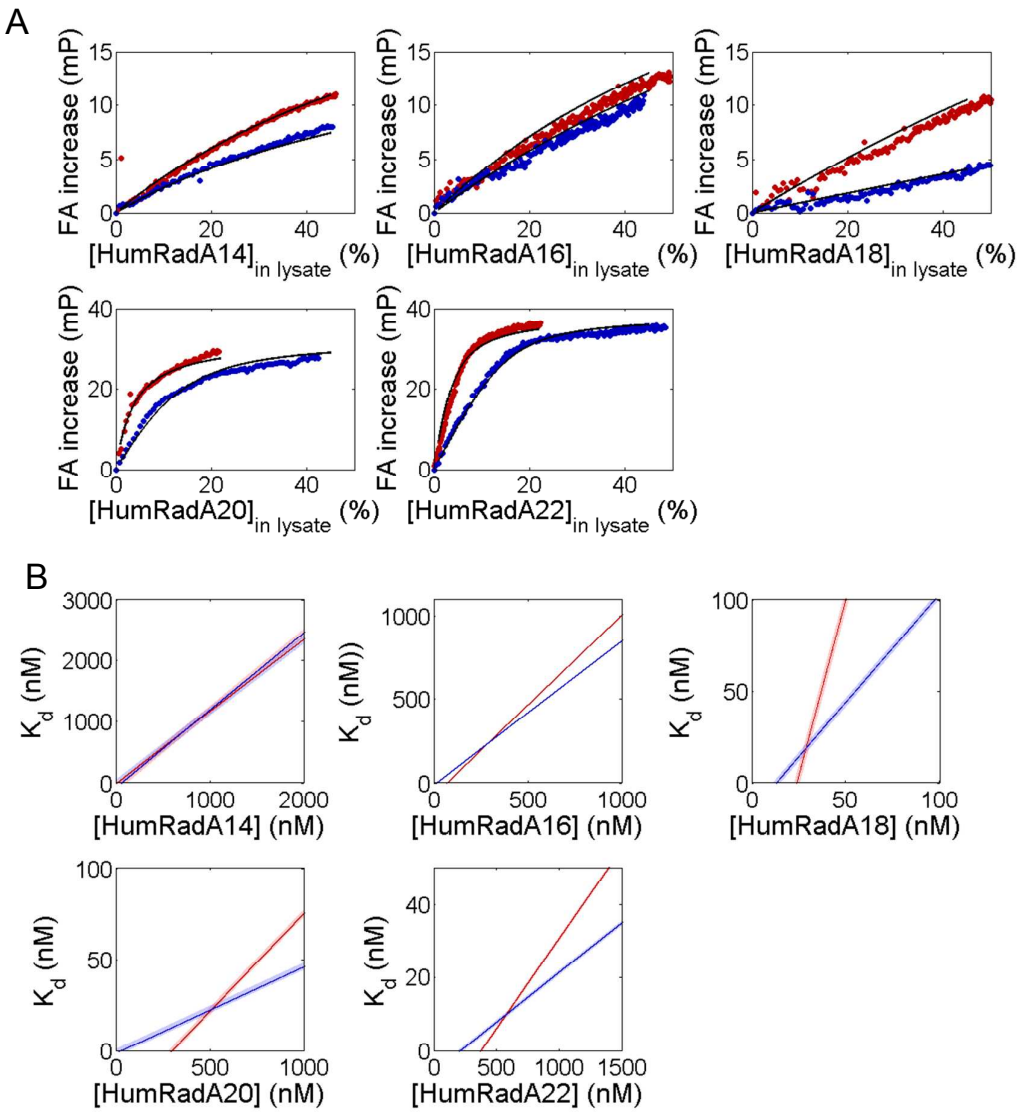

Figure S10. *Cell lysate screens in nanoliter droplets: two titrations were performed for each HumRadA variant* (**A**) Titration data and overlaid fits for the HumRadA variants binding $BRC4^{fl}$ in lysate solutions. (**B**) Unique correlations for each variant extracted from the fitting parameters from (A).

S11. Fitting for the competition assay

The competition curves were plotted using the following equation to transform anisotropy readings into percentage of binding:

$$F_b = S_b + \frac{A - A_0}{A_{\max}} \qquad \text{(eq. S2)}$$

Where F_b is the fraction of labelled BRC4 bound, S_b is the starting fraction bound, A, A_0, the anisotropy values for each point and the first point in the titration respectively, A_{max} is the maximum difference observed between fully bound and fully unbound ligands (34 mP). Here, S_b was the initial bound fraction.

S12. Analytical formula for the competition assay

After converting anisotropy values into bound fraction, the affinity of the competitor was found using a complete competitive binding model.
The unlabelled peptide MBP-BRC4 competes with the labelled BRC4^{fl} for binding unlabelled HumRadA18 proteins. The bound fraction F_b can be related to dissociation constants of both labelled and unlabelled peptides (K_d^1, K_d^2) using the following formulae:

$$F_b = \frac{2\sqrt{(d^2 - 3e)}\cos(\vartheta/3) - d}{3K_{d1} + 2\sqrt{(d^2 - 3e)}\cos(\vartheta/3)} - d \quad \text{(eq. S3)}$$

$$d = K_{d1} + K_{d2} + BRC4 - fl + BRC4 - MBP - V_{18}$$
$$e = (BRC4 - MBP - V_{18})K_{d1} + (BRC4 - fl\ - V_{18)}K_{d2} + K_{d1}K_{d2}$$
$$f = -K_{d1}K_{d2}V_{18}$$

$$\vartheta = \arccos\left[\frac{-2d^3 + 9de - 27f}{2\sqrt{(d^2 - 3e)^3}}\right]$$

The corresponding Matlab script is given below:

```
clear all;

close all;

Vt=60;% concentration of HumRadA18 in nM

Kd1=45; % kd for BRC4fl – HumRadA18

 Kd2=110; % kd for MBP-BRC4-HumRadA18
```

```
BRC3=(0:1:1000); % concentration range for MBP-BRC4

BRC4=40; % concentrations of BRC4fl

 d=Kd1+Kd2+BRC4+BRC3-Vt;

 e=(BRC3-Vt).*Kd1+(BRC4-Vt).*Kd2+Kd1.*Kd2;

 f=-Kd1.*Kd2.*Vt;

 theta=acos((-2.*d.^3+9.*d.*e-27.*f)./(2.*sqrt((d.^2-3.*e).^3)));

 Fsb=(2.*sqrt(d.^2-3.*e).*cos(theta./3)-d)./(3.*Kd1+2.*sqrt(d.^2-3.*e).*cos(theta./3)-d);

semilogx(BRC3,Fsb,'Color','red');
```

S13. Fluorescence Polarization Assay in Microplates

For comparison of measurements in droplets with a conventional experimental set-up, experiments were carried in a microplate reader:
Fluorescence Polarisation binding and competition experiments were performed at 25 °C in 100 mM Tris pH 7.5, 200 mM KCl, 1.25% v/v glycerol. The samples were loaded onto Costar 96-well half-area black microplates and fluorescence data were recorded using a PheraStar plate reader (BMG) equipped with polarisation filters ($\lambda_{excitation}$ 485 nm, $\lambda_{emission}$ 520 nm). The concentration of Alexa Fluor 488-labelled BRC4 peptide was constant at 10 nM and the concentration of each protein titrant was adjusted based on the dissociation constant observed in trial experiments.

S14. Materials

S14.1 Expression of HumRadA proteins

The HumRadA proteins contain rare Arg codons, thus the helper plasmid pUBS520 (KanR) was used for coding the corresponding rare tRNAs. HumRadA18 was produced in BL21(DE3). The BL21(DE3) pUBS520 cells were transformed with the pBAT plasmids (AmpR).[6] A LB pre-culture (10 mL) with appropriate antibiotics was prepared inoculated from a single colony and incubated overnight at 37 °C with shaking (230 rpm). LB (500 mL) containing antibiotics (ampicillin 100 μg/mL, kanamycin 20 μg/mL) was inoculated with the overnight culture and incubated at 37 °C, 200 rpm for several hours until an $A_{600\,nm}$ of 1 was reached. The cells were induced with IPTG (400 μM) and incubated for 4 hours at 37 °C under shaking (210 rpm) after which the cells were harvested. Cell pellets were re-suspended in MES (15 mL; 20 mM, pH 6.0) and stored at -20 °C. For protein purification the cells were sonicated at a 50% amplitude with 10 seconds intervals for a total sonication time of 6 minutes. The solution was centrifuged (30 min, 6,000 rpm at 4°C) and the supernatant purified by ion exchange chromatography. After loading onto a HiTrap SP-Sepharose HP column (5 mL; equilibrated in 20 mM MES, pH 6.0, containing 0.5 mM EDTA). Elution of HumRadA was brought about by a NaCl concentration gradient (0 to 500 mM in 500 mL, buffer as above). Fractions containing HumRadA (eluting ~300 mM NaCl) were pooled and loaded on a size exclusion column (Superdex 75 16/60), which was previously equilibrated in 20 mM MES pH 6.0, 1 mM EDTA, 200 mM Arg. Fractions identified by SDS/PAGE to contain the desired proteins were pooled and stored at 4 °C.
The protein concentration was determined by diluting the protein sample in 6 M guanidinium chloride, 50 mM sodium phosphate pH 7.5 and recording an absorbance spectrum from 340 – 220 nm. Absorbance at 280 nm was corrected by subtracting the background absorbance at 320 nm and converted to a concentration using a molar extinction coefficient of 8,920 $cm^{-1}M^{-1}$ (calculated using the Edelhoch method[7]).

S14.2 Preparation of peptides

BRC4 was synthesised by the PNAC Service (Department of Biochemistry) using standard FMOC chemistry. BRC4 was acetylated in the N-terminus and amidated in the C-terminus and had the sequence Ac-CKEPTLLGFHTASGKKVKIAKESLDKVKNLFDEKEQ-NH2. Fluorescently labeled $BRC4^{fl}$ repeat was prepared by reacting the synthetic peptide with an excess of maleimide-fluorescein dye, followed by reverse phase chromatography using 4.6 x 250 mm Ace C18 300Å column, giving a purity above 99%.

S14.3 Humanizing mutations in different HumRadA variants[6]

Mutant	Mutations
HumRadA14	V168A, I169M, W170Y, Y201A, V202Y, L213Q, V215L, Q216Y, E219S, D220A, K221M, I222M, K223V, L225S, V232Y, H264F, D267M, L274E, Y275F
HumRadA16	V168A, I169M, W170Y, Y201A, V202Y, L213Q, V215L, Q216Y, E219S, D220A, K221M, I222M, K223V, L225S, V232Y, K263R, H264F, A266R, D267M, L274E, Y275F
HumRadA18	V168A, I169M, W170Y, K198D, H199N, I200V, Y201A, V202Y, L213Q, V215L, Q216Y, E219S, D220A, K221M, I222M, K223V, L225S, V232Y, K263R, H264F, D267M, L274E, Y275F
HumRadA20	V168A, I169M, W170Y, K198D, H199N, I200V, Y201A, V202Y, L213Q, V215L, Q216Y, E219S, D220A, K221M, I222M, K223V, L225S, V232Y, K263R, H264F, A266R, D267M, L274E, Y275F
HumRadA22	V168A, I169M, W170Y, I182L, K198D, H199N, I200V, Y201A, V202Y, L213Q, V215L, Q216Y, E219S, D220A, K221M, I222M, K223V, L225S, V232Y, K263R, H264F, A266R, D267M, L274E, Y275F

Supplementary References

(1) McDonald, J. C., Duffy, D. C., Anderson, J. R., Chiu, D. T., Wu, H., Schueller, O. J. A., Whitesides, G. M., *Electrophoresis.* 2000. 27-40.

(2) Mazutis, L., Gilbert, J., Ung, W. L., Weitz, D. A., Griffiths, A. D., Heyman, J. A., *Nat Protocols*. 2013, 8. 870-91.

(3) Xia, Y., Whitesides, G. M., *Annu. Rev. Mater. Sci.* 1998, 28. 153-84.

(4) Zinchenko, A., Devenish, S. R., Kintses, B., Colin, P. Y., Fischlechner, M., Hollfelder, F., *Anal. Chem*. 2014, 86. 2526-2533.

(5) Skhiri, Y., Gruner, P., Semin, B., Brosseau, Q., Pekin, D., Mazutis, L., Goust, V., Kleinschmidt, F., El Harrak, A., Hutchison, J. B., Mayot, E., Bartolo, J. F., Griffiths, A. D., Taly, V., Baret, J. C., *Soft Matter.* 2012, 8. 10618-10627.

(6) Moschetti, T., Sharpe, T.,Fischer, G., Marsh, M., Ng, H., Morgan, M., Scott, D., Blundell, T. L., Venkitaraman, A., Abell, C., Hyvonen, M., *J Mol Biol.* 2016, submitted.

(7) Pace, C. N., Vajdos, F., Fee, L., Gray, T., *Protein Sci.* 1995, 4. 2411–2423.